

Electronic Supplementary Information

Cerium-based UiO-66 Metal-organic Frameworks Explored as Efficient Redox Catalyst: Titanium Incorporation and Generation of Abundant Oxygen Vacancies

Yajun Zhang,^{‡a} Hanjiao Chen,^{‡a} Xiaoliang Zeng,^a Yi Pan,^{a,c} Xiaofang
Jiang,^a Zhou Long,^{a*} Xiandeng Hou^{a,b}

^aAnalytical & Testing Center, Sichuan University, Chengdu 610064, China;

^bDepartment of Chemistry, Sichuan University, Chengdu 610064, China.

*^cInstitute of Chemistry, National Institute of Measurement and Testing Technology,
Chengdu 610021, China.*

[‡] Yajun Zhang and Hanjiao Chen contributed equally to this work.

* To whom correspondence should be addressed. E-mail: longzhou@scu.edu.cn

Telephone: +86-137-3084-2563

Materials and experimental details

1 Reagents and materials

Cerium ammonium nitrate ($(\text{NH}_4)_2\text{Ce}(\text{NO}_3)_6$), terephthalic acid (H_2BDC), 2-hydroxy-1,4-benzenedicarboxylic acid (BDC-OH), titanocene dichloride (TiCp_2Cl_2), titanium dioxide (TiO_2 5-10 nm in particle size), cerium dioxide (CeO_2 20-50 nm in particle size), tetracycline (TC), and 5,5-Dimethyl-1-pyrroline N-oxide (DMPO, 97%) were purchased from Aladdin Reagents Co. Ltd. (Shanghai, China). Sodium selenate was obtained from Xiya Chemical Industry Co. Ltd. (Shandong, China). N, N-Dimethylformamide (DMF), ethanol, formic acid (HCOOH) were obtained from Kelong Chemical Reagent Co. Ltd. (Chengdu, China). All chemicals were at least AR grade and used without further treatment. Ultrapure water ($18.25 \text{ M}\Omega\cdot\text{cm}$) used for all experiments was obtained from a water purification system (PCWJ-10, Pure Technology Co. Ltd, Chengdu, China).

2 Synthesis of UiO-66(Ce)

H_2BDC (212.4 mg, 1.3 mmol) was mixed well with 7.5 mL DMF in a 20 mL round-bottom flask. The aqueous $(\text{NH}_4)_2\text{Ce}(\text{NO}_3)_6$ (2.4 mL, 0.5333 M) was added in under stirring to obtain a homogeneous solution. The flask was sealed and heated using an aluminum heater block under stirring for 30 min at 100 °C. A light yellow precipitate was obtained, collected by centrifugation, and then washed with DMF and ethanol, each for three times. The resulting powders of UiO-66(Ce) crystals were collected from ethanol by centrifugation and then dried under vacuum at 80 °C before use.

3 Synthesis of UiO-66(Ce/Ti)

The TiCp_2Cl_2 (97.5 mg, 0.4 mmol equiv based on Ti) and the UiO-66(Ce) crystals (130 mg, 0.4 mmol equiv based on Ce) were mixed in 25 mL DMF with vigorous stirring. The obtained uniform slurry was transferred to a 50 mL round-bottom flask, and kept at 100 °C for 3 h (unless mentioned otherwise) and then cooled down to the ambient temperature. The product, UiO-66(Ce/Ti), was collected by centrifugation and washed with DMF and ethanol, each for three times. The resultant UiO-66(Ce/Ti) crystals were collected from ethanol by centrifugation and then dried under vacuum at 80 °C before use.

4 Characterization

The PXRD patterns were collected by an EMPYREAN (Panalytical Inc., Netherlands) with a $\text{Cu K}\alpha$ radiation. The morphology of the samples was observed by a field emission scanning electron microscope (SEM) (Hitachi, Japan), and the elemental mapping was accomplished by the energy dispersive X-ray spectroscope (EDS) coupled to the SEM. The thermal stability study on 5-10 mg of UiO-66(Ce) or UiO-66(Ce/Ti) crystals was performed with a DSC1 thermogravimetric analyzer (Mettler Toledo, Switzerland) from 30 °C to 600 °C at a rate of $50 \text{ mL}\cdot\text{min}^{-1}$ under air flow. The X-ray photoelectron spectroscopy (XPS) spectra were collected with an AXIS Ultra

DLD 800 X (Kratos, UK). The Brunauer-Emmett-Teller surface areas (S_{BET}) were measured based on a N_2 adsorption isotherm using a Micromeritics ASAP 2460 (4356 Communication Dr., Norcross, Ga 30093-2901 USA) at 77 K. The photoluminescence spectra and further lifetime measurements were performed on an Fluorolog-3 spectrofluorometer (Horiba Jobin Yvon), with a picosecond photo detection module (PPD-850, Horiba Scientific) as the detector. The content of titanium in UiO-66(Ce/Ti) samples was analyzed by inductively coupled plasma-optical emission spectrometer (ICP-OES, ARCOS FHS12, SPECTRO Analytical Instruments Inc., Germany). Before the analysis by ICP-OES, each kind of solid sample was digested in a 5-mL mixture of HNO_3 and HCl (v/v=7:3) and heated at 150 °C for 2 h. 1 mL H_2SO_4 and 0.5 g $(\text{NH}_4)_2\text{SO}_4$ was added in and the mixture was kept heating until turning clear. For the Kubelka-Munk method, the UV-vis diffuse reflectance spectra (DRS) were collected from a dry-pressed disk samples by a UV-3600 spectrometer (Shimazu, Japan), with BaSO_4 as the reflectance standard.

5 Photoelectrochemical analysis

The Mott-Schottky curves were obtained by using an Autolab PGSTAT12 potentiostat/galvanostat (Metrohm, Switzerland) in a three-electrode cell. A Pt plate was used as the counter electrode and a Ag/AgCl electrode (3M KCl) was used as the reference electrode, with a solution of 0.1 M Na_2SO_4 as the electrolyte. To prepare the working electrodes, FTO glass was ultrasonically cleaned in soap suds, deionized water, and acetone successively. The working electrode was prepared on fluorine-doped tin oxide (FTO) glass, with a slurry mixture containing 5 mg sample, 375 μL water, 125 μL isopropanol, 10 μL nafion dipped on the surface. The area of the electrodes is about 1x1 cm^2 . The electrochemical impedance measurement was performed by using an CHI-660 electrochemical workstation (Chinstruments, China) in a three-electrode system with 0.1 M Na_2SO_4 as the electrolyte. The photocurrent measurement was performed by using the same workstation. For the fabrication of the UiO-66 electrodes, 20 mg UiO-66(Ce)/UiO-66(Ce/Ti) nanoparticles were dispersed in 20 mL chitosan solution and then exposed to ultrasound for homogeneity purpose. The obtained uniform suspension was spin-coated onto ITO glass and dried in an oven for overnight.

A 500 W iodine tungsten lamp was used as the stimulated sunlight source for all the photocatalytic experiments unless mentioned otherwise.

The calculated band gaps of UiO-66 (Ce) and UiO-66(Ce/Ti) were determined to be 2.95 eV and 2.84 eV, respectively, according to the diffuse reflectance UV-Vis spectra (Figure S8). Based on the Mott-Schottky plots (Figure S9) the slope was consistent with typical n-type semiconductors¹. The flat band potential obtained from the intercept was approximately -0.60 V vs. Ag/AgCl (i.e. -0.40 V vs NHE (Normal Hydrogen Electrode)) for UiO-66 (Ce), and -0.50 V vs Ag/AgCl (i.e. -0.30 V vs. NHE) for UiO-66(Ce/Ti)². Moreover, for common n-type semiconductors, it is generally believed that the bottom of the conduction band is more negative than the flat band potential by about 0.10 V¹ so the conduction band (CB) of UiO-66 and UiO-66(Ce/Ti) can be estimated to be -0.50 V and -0.40 V vs. NHE, respectively, and the valence band

(VB) was calculated to be 2.45 V and 2.44 V, respectively.

6 Analysis of reactive oxygen species

The electron paramagnetic resonance (EPR) spectra of superoxides anions, hydroxyl radicals, or oxygen vacancies, spin-trapped by 5,5-dimethyl-1-pyrroline N-oxide (DMPO), were collected at room temperature by using a BRUKER EPR spectrometer (EXM, Germany). The sample was composed of 20 μL MOFs suspension ($5 \text{ mg}\cdot\text{mL}^{-1}$), 10 μL DMPO and 1 mL water, and irradiated for 5 min before the EPR measurement.

For the $^1\text{H-NMR}$ measurement, 5 mg MOFs sample was dispersed in 2 mL water irradiated by the light source for 30 min and then dried at $100\text{ }^\circ\text{C}$ for 24 h. The BDC-OH or the resulting sample was digested in DMSO (500 μL) and HF (20 μL , 40% aqueous solution) under ultrasound until the measurement.

7 Photocatalytic redox experiments

For the degradation of TC, 1.5 mg MOFs as the photocatalysts were homogeneously dispersed in 15 mL TC solution (30 mg/L) by stirring in the dark to reach the equilibrium of adsorption-desorption. The mixture was then exposed to the light source under continuous stirring. Once the light illumination began, 0.5 mL of each sample was collected from the suspension at an interval of 10 min, with the supernatant obtained after centrifugation analyzed instantly by UV-vis.

For the photo-reduction of Se(VI), 2.0 mg MOFs as the photocatalysts was dispersed in 5 mL formic acid (20 % aqueous solution) to form a homogeneous suspension. Then the suspension was pumped into a quartz pipe under the light irradiation. The product of the photocatalytic process was analyzed by atomic fluorescence spectrometry with an AFS-9700 spectrometer (Beijing Haiguang Instrument Inc., China) using the operation parameters listed in Table 5.

All the photocatalytic experiments were carried out at room temperature.

Tables

Table S1 Physicochemical properties³

Sample	S_{BET} (m ² /g) ^a	S_{micro} (m ² /g) ^b	S_{meso} (m ² /g) ^c	$S_{\text{meso}}/S_{\text{micro}}$	V (cc/g) ^d	D (nm) ^e
UiO-66(Ce)	863.75	784.12	79.62	0.102	0.32	0.66
UiO-66(Ce/Ti)	1032.86	864.88	167.98	0.194	0.48	0.78

^a Brunauer-Emmett-Teller (BET) surface area

^b Micropore surface area calculated using the t-plot method

^c Mesopore surface area calculated using the t-plot method

^d Total pore volume measured at $P/P_0 = 0.99$

^e Median pore width

Table S2 XPS peak assignment, peak area and calculated content for Ce³⁺ and Ce⁴⁺

Species	UiO-66(Ce)			UiO-66(Ce/Ti)		
	Binding energy (eV)	Peak Area	Content (%) ^a	Binding energy (eV)	Peak Area	Content (%) ^a
Ce ³⁺	881.1	525.3	35.83	880.8	403.2	43.95
	885.7	4407.5		885.0	2638.7	
	899.1	3000.8		899.1	900.3	
	903.9	2518.5		903.6	1600.0	
Ce ⁴⁺	883.0	3733.0	64.17	882.5	1916.0	56.05
	888.0	4860.2		886.5	1961.4	
	898.3	1641.2		898.1	499.4	
	901.5	3082.2		901.3	802.6	
	907.3	2000.0		905.6	1280.2	
	917.1	3402.4		916.7	608.1	

^a Based on the previous articles⁴ about Ce3d XPS in UiO-66(Ce) and CeO₂, which also involved peak designation and calculation of Ce species in content, the content(%) was calculated based on the peak areas of all peaks for Ce³⁺ or Ce⁴⁺ divided by the peak areas of all the ten peaks for both Ce³⁺ or Ce⁴⁺ in UiO-66(Ce) or UiO-66(Ce/Ti).

Table S3 Surface oxygen composition and states determined by XPS

Sample	Binding Energy (eV)	Surface Oxygen (O) Species	Peak Area	Content (%) ^a
UiO-66(Ce)	532.6	absorbed O	6793.9	30.9
	531.3	O in BDC ligand ⁵	13630	61.9
	529.5	lattice O	1592.5	7.2
UiO-66(Ce/Ti)	533.3	O vacancy	1805.6	5.6
	531.3	O in BDC ligand ⁵	19250	59.8
	529.9	lattice O	11114.1	34.6

^a The content(%) was calculated based on the peak area of the specific peak divided by the peak areas of the three peaks for the three oxygen species in UiO-66(Ce) or UiO-66(Ce/Ti) as the previously reported⁶.

Table S4 Photoluminescent lifetime determination

Sample	$\bar{\tau}/ns^a$	τ_i/ns^b	f_i	$\chi^2 R$
Ui0-66(Ce)	26.9	1.67 ± 0.006	0.39	1.35
		43.1 ± 0.005	0.61	
Ui0-66(Ce/Ti)	20.7	1.68 ± 0.006	0.53	1.76
		42.6 ± 0.006	0.47	

a: The fluorescence {P decay was fitted to the second order exponential decay.

b: The retrieved lifetime was calculated with the standard deviation as error.

The average fluorescence lifetime was calculated using the equation:

$$\bar{\tau} = \sum f_i \tau_i = f_1 \tau_1 + f_2 \tau_2 + f_3 \tau_3$$

where τ_i is the lifetime and f_i is the contribution factor of τ_i to τ , which were collected from the fluorescence lifetime measurements after proper fitting.

Table S5 The optimal parameters of AFS

PMT voltage	-300 V
HLC current	90 mA
Auxiliary current	45 mA
Argon flow rate	300 mL•min ⁻¹
Hydrogen flow rate	60 mL•min ⁻¹
Irradiation time	30 s

Figures

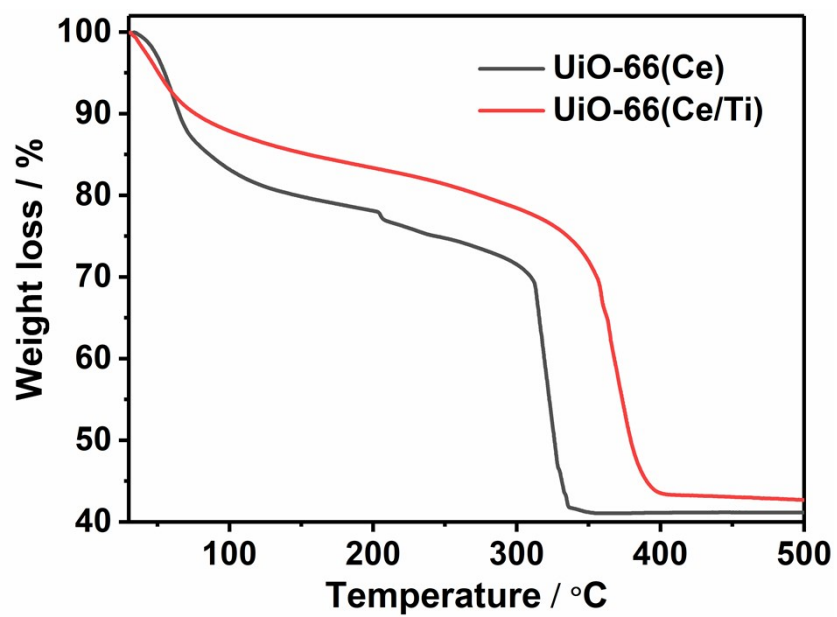


Figure S1 TGA curve obtained from UiO-66(Ce) and UiO-66(Ce/Ti).

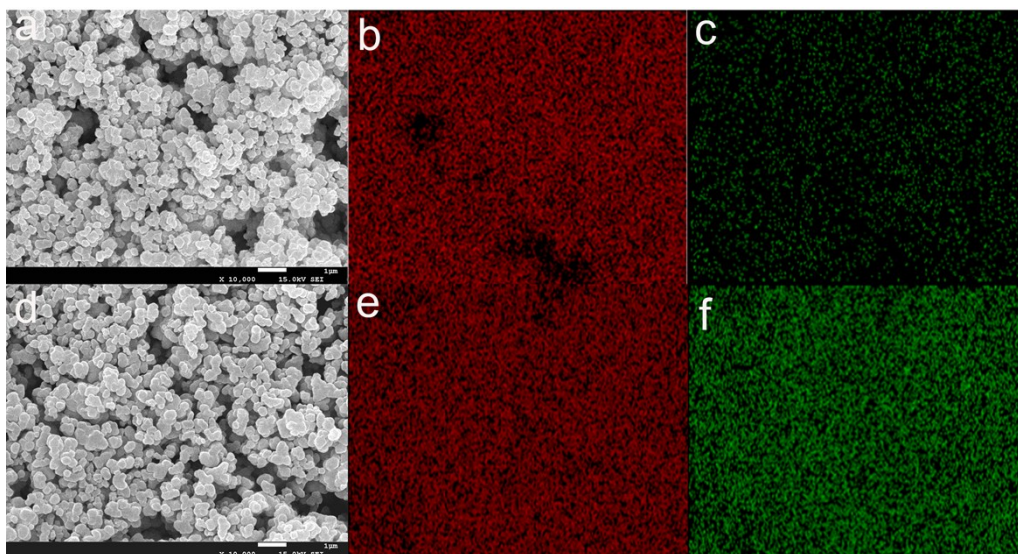


Figure S2 SEM image of UiO-66(Ce) (a) and UiO-66(Ce/Ti) (d); energy-dispersed X-ray mapping of Ce obtained from UiO-66(Ce) (b) and UiO-66(Ce/Ti) (e); energy-dispersed X-ray mapping image of Ti obtained from UiO-66(Ce) (c) and UiO-66(Ce/Ti) (f).

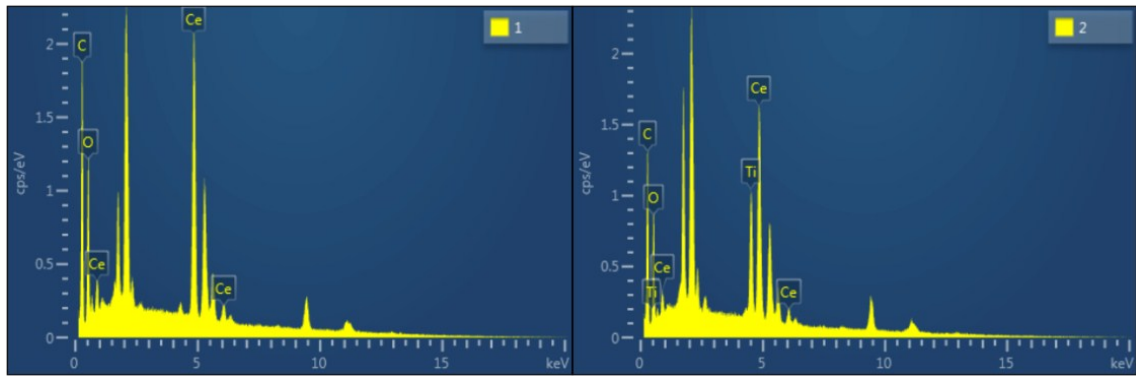


Figure S3 Energy dispersive X-ray spectroscopy (EDS) results obtained from UiO-66(Ce) (left) and UiO-66(Ce/Ti) (right).

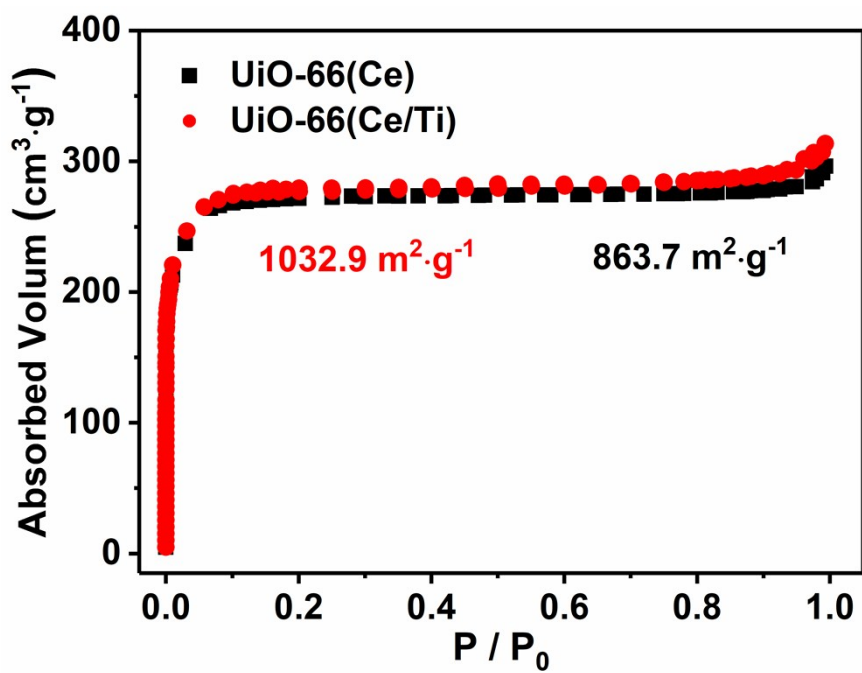


Figure S4 N₂ adsorption/desorption isotherm of UiO-66(Ce) and UiO-66(Ce/Ti) and accordingly obtained surface area as the previously reported³.

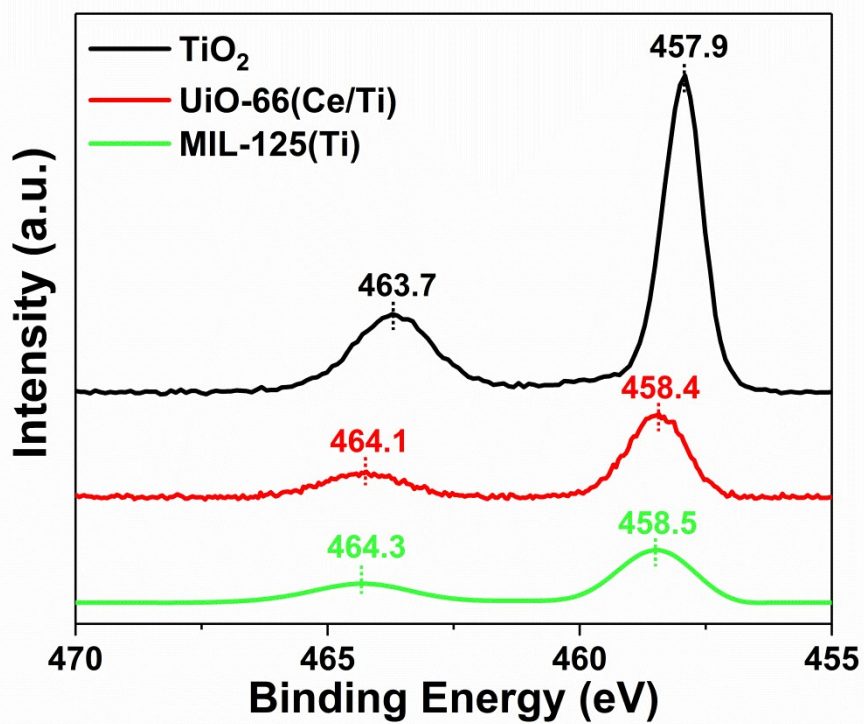


Figure S5 Ti_{2p} XPS spectra of UiO-66(Ce/Ti), MIL-125(Ti) and TiO₂.

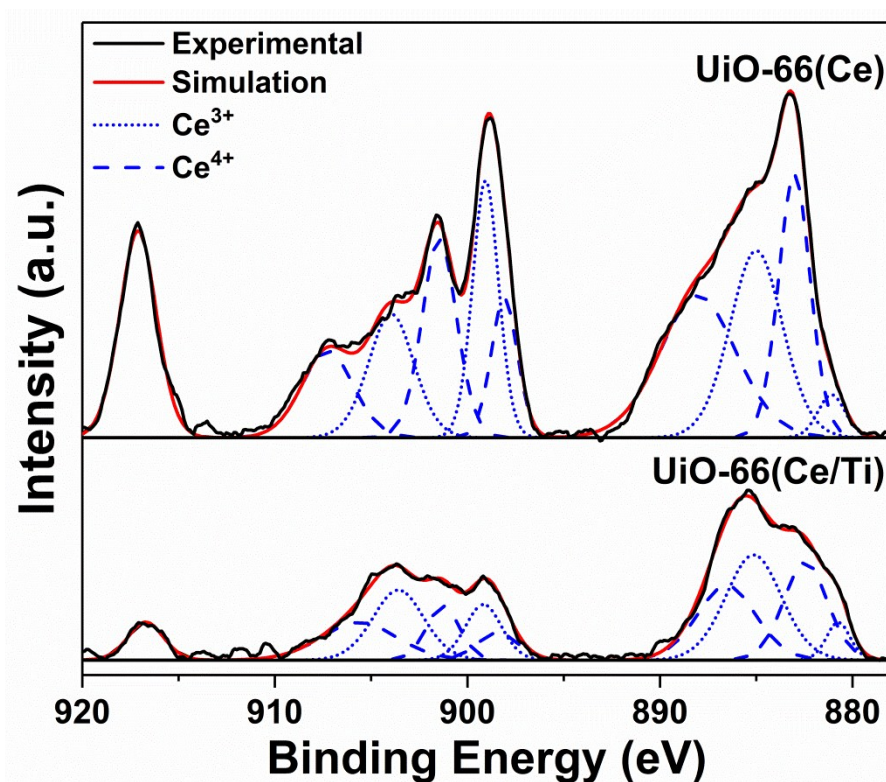


Figure S6 XPS spectra in the Ce core level region obtained from UiO-66(Ce) and UiO-66(Ce/Ti), deconvoluted as the previously reported^{4a, 4b}.

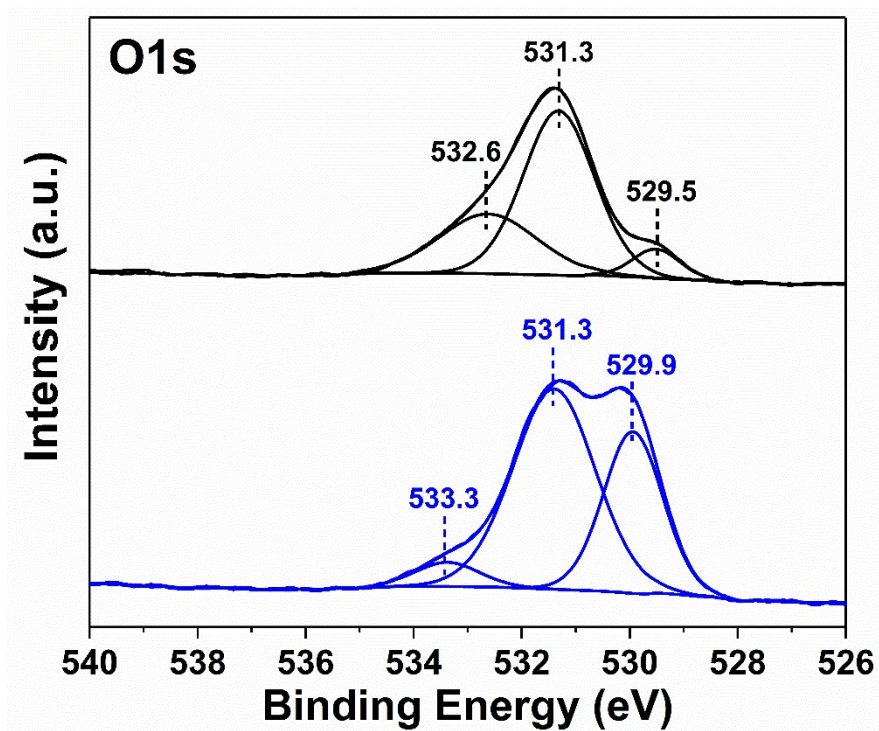


Figure S7 O1s XPS spectra collected from UiO-66(Ce) (top) and UiO-66(Ce/Ti) (bottom)^{4b}, deconvoluted as the previously reported^{4a}.

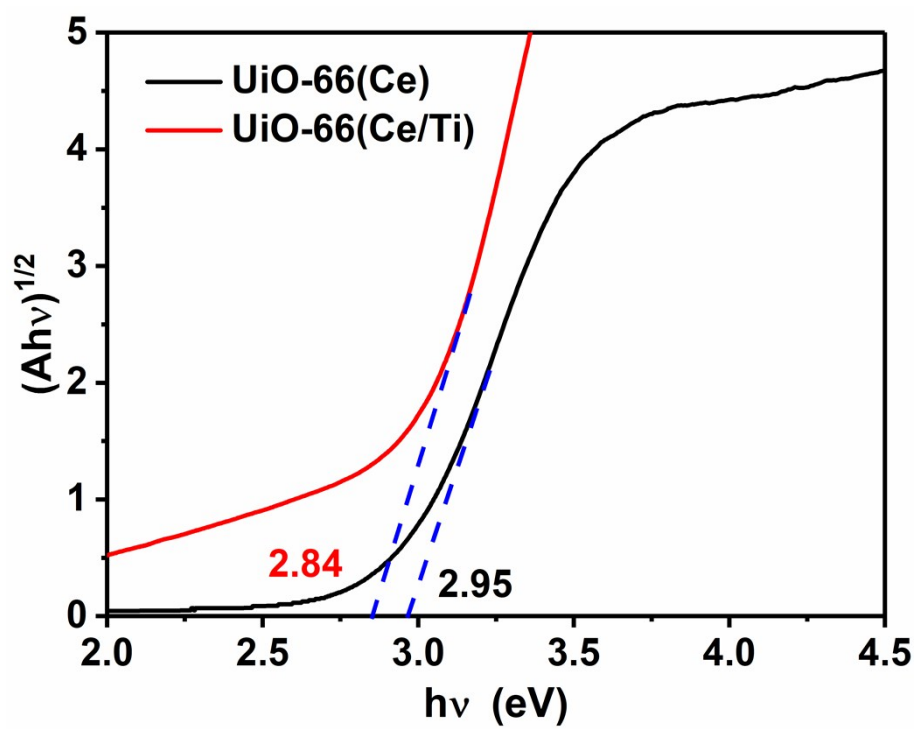


Figure S8 Diffuse reflectance UV-Vis spectra of UiO-66(Ce) and UiO-66(Ce/Ti).

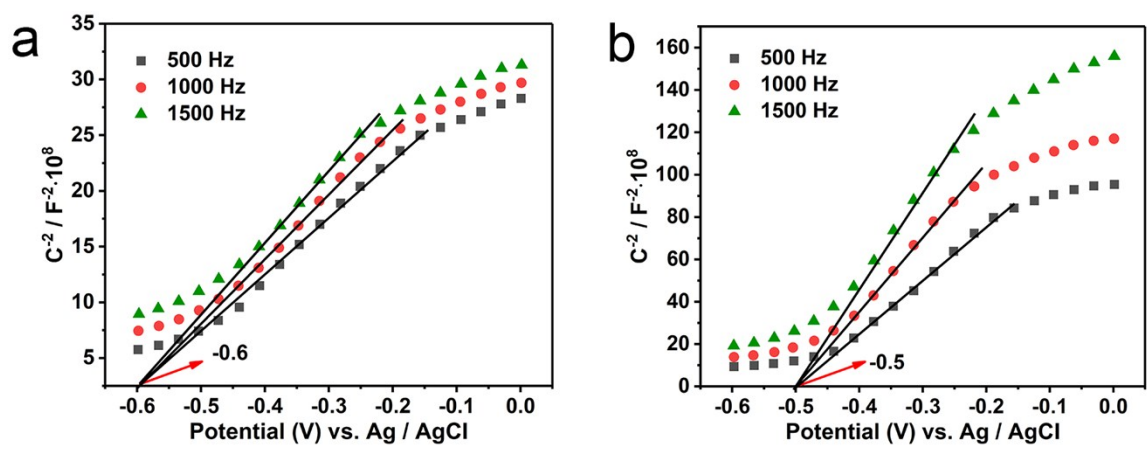


Figure S9 Mott-Schottky plot obtained from UiO-66(Ce) (a) and UiO-66(Ce/Ti) (b).

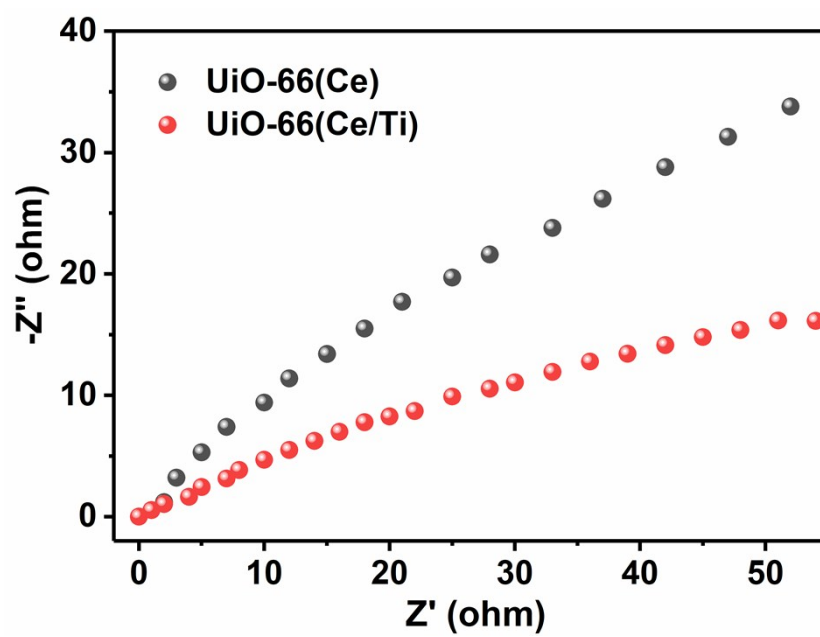


Figure S10 EIS curve obtained from $UiO-66(Ce)$ and $UiO-66(Ce/Ti)$.

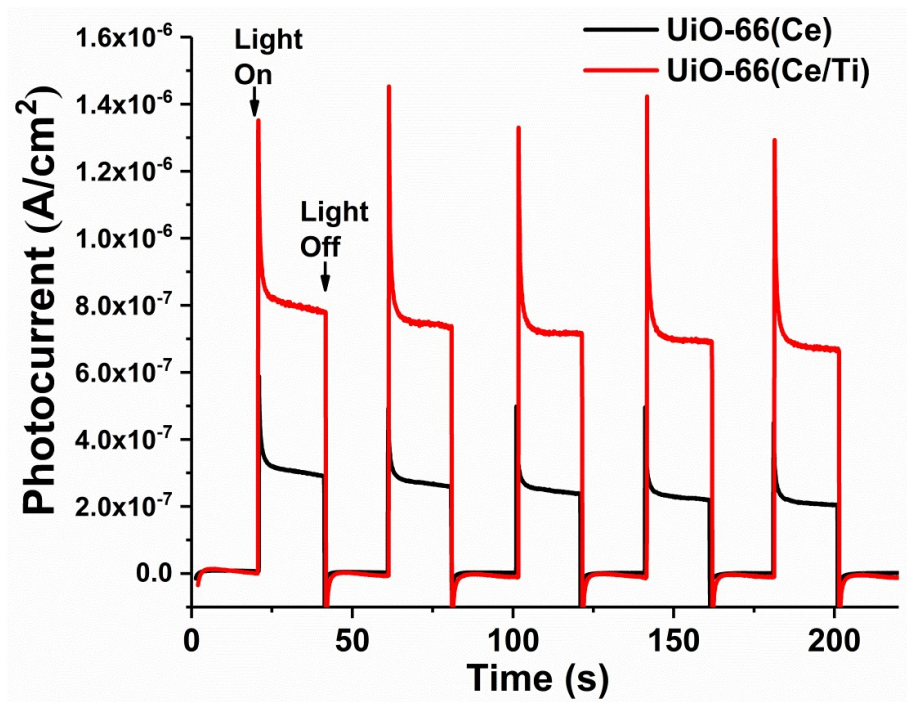


Figure S11 Photocurrent response obtained from UiO-66(Ce) and UiO-66(Ce/Ti) under the irradiation of simulated sunlight

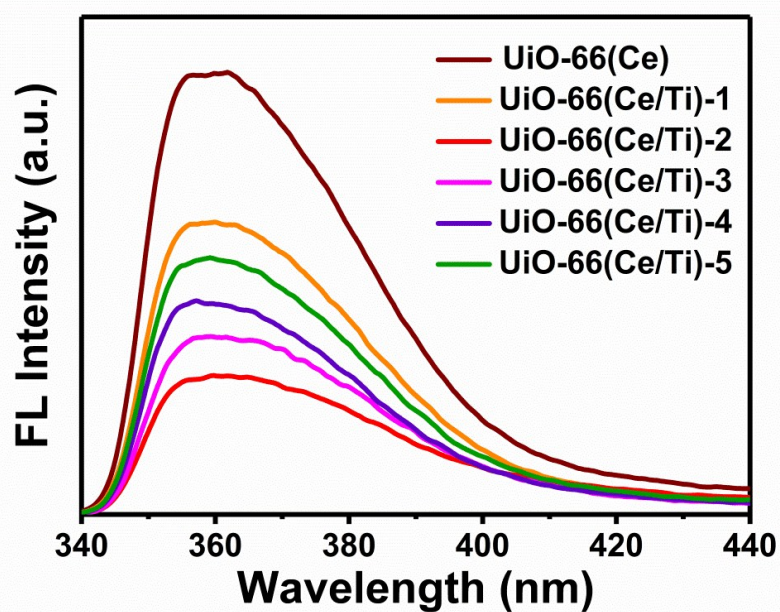


Figure S12 Under the irradiation of simulated sunlight the collected spectra of PL derived from the emission of BDC-ligand in UiO-66(Ce) and UiO-66(Ce/Ti) synthesized by the reaction between UiO-66(Ce) and TiCp_2Cl_2 at 100 °C for 2 h ((UiO-66(Ce/Ti)-1), 3 h ((UiO-66(Ce/Ti)-2), 4 h ((UiO-66(Ce/Ti)-3), 5 h ((UiO-66(Ce/Ti)-4) and 24 h ((UiO-66(Ce/Ti)-5), respectively.

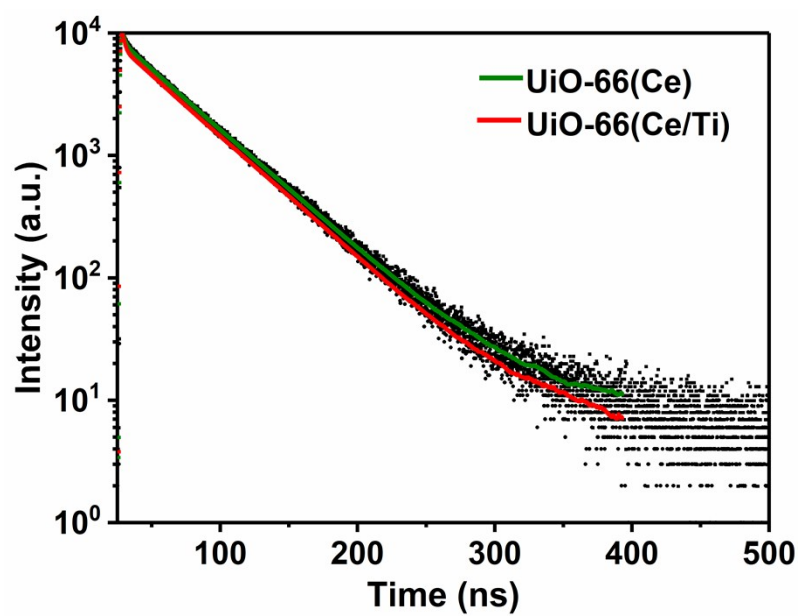


Figure S13 Fluorescence decay curves of UiO-66(Ce) and UiO-66(Ce/Ti)

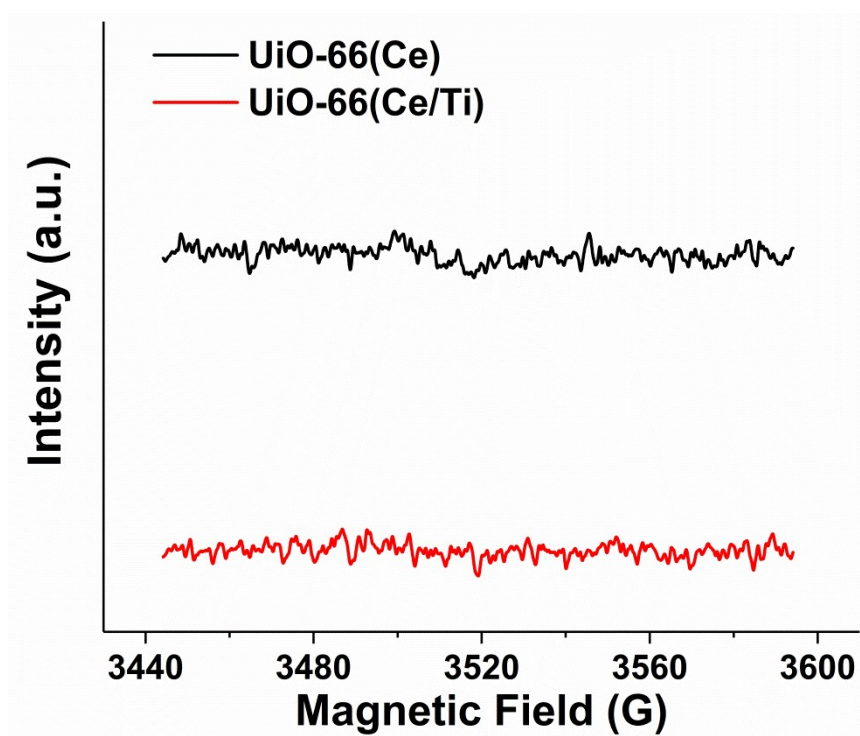


Figure S14 EPR spectra obtained after sunlight irradiation to UiO-66(Ce) and UiO-66(Ce/Ti) for $\cdot\text{OH}$ detection

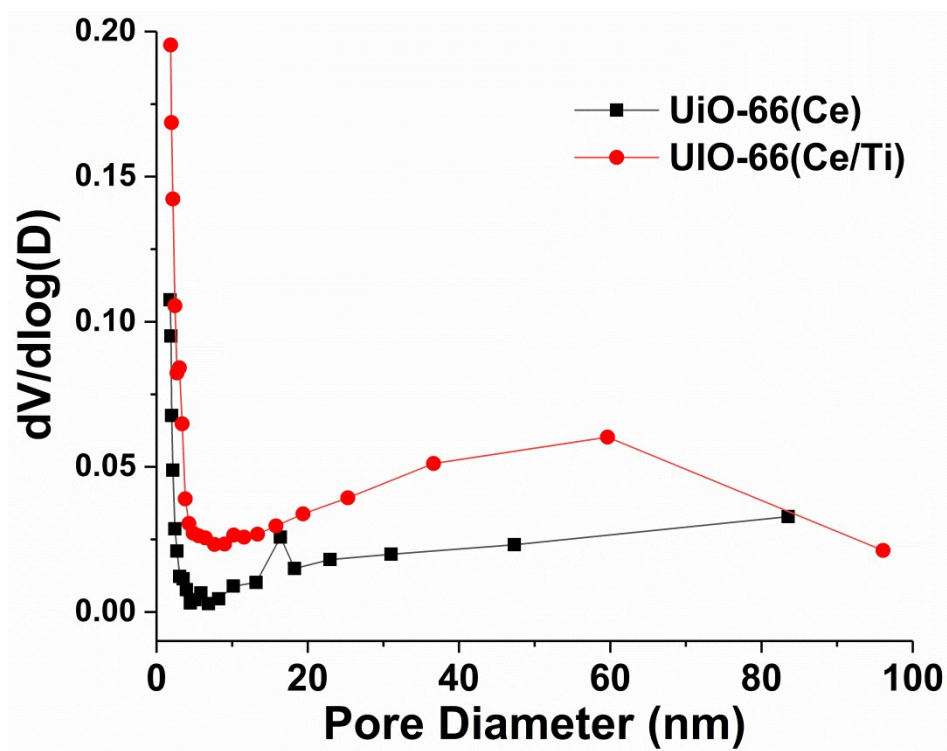


Figure S15 BJH pore size distribution curves of UiO-66(Ce) and UiO-66(Ce/Ti)

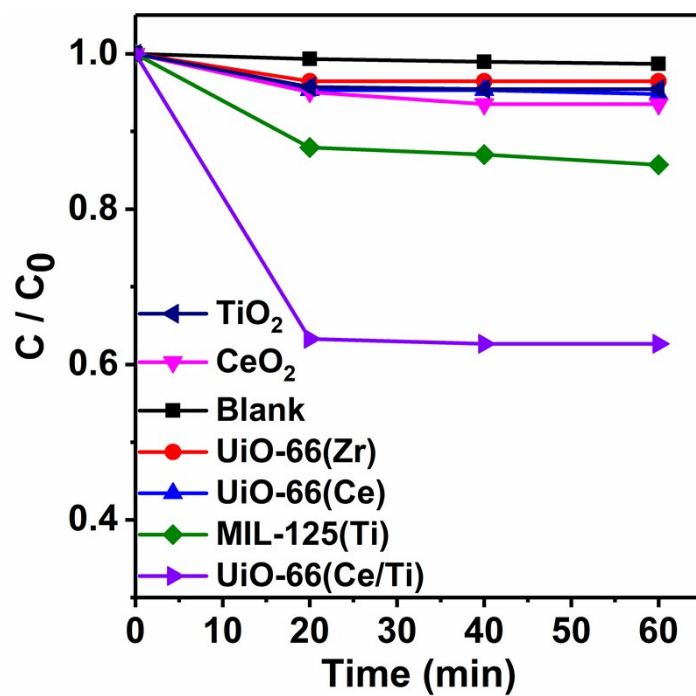


Figure S16 Time-evolving ab/desorption curve for TC in the dark obtained by using different catalysts.

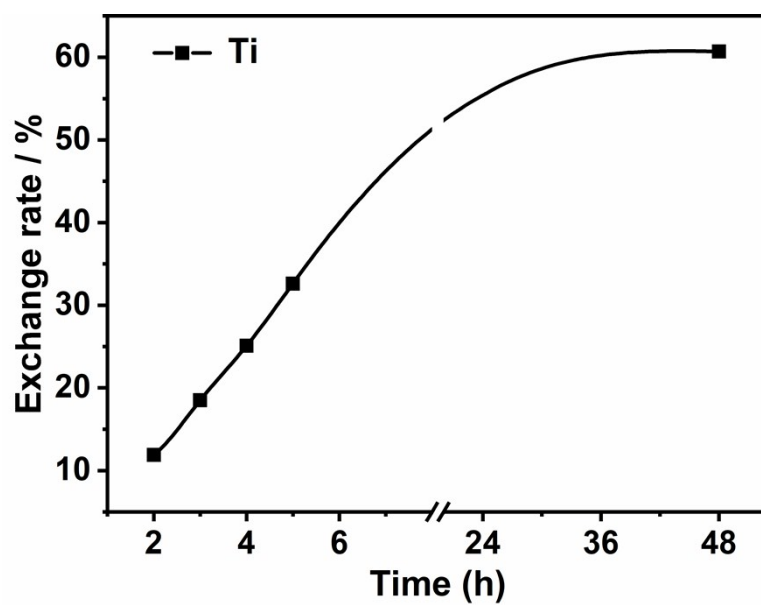


Figure S17 Percentage of the incorporated Ti to UiO-66(Ce) after the reaction with TiCp_2Cl_2 for different periods of time, which was determined by inductively coupled plasma optical emission spectrometry.

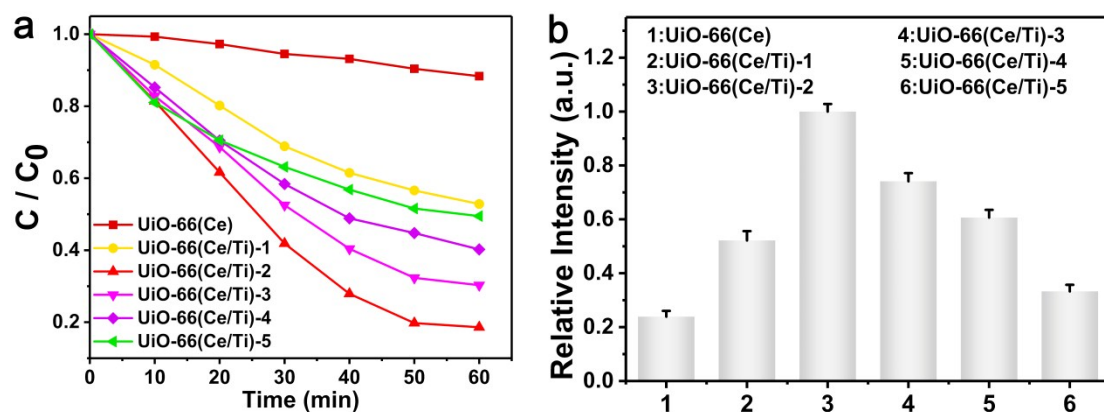


Figure S18 Time-evolving curve for TC degradation (left) and AFS signal intensity of Se reduced from Se(VI) (right) by using UiO-66(Ce) and UiO-66(Ce/Ti) synthesized by the reaction between UiO-66(Ce) and TiCp_2Cl_2 at 100 °C for 2 h ((UiO-66(Ce/Ti)-1), 3 h ((UiO-66(Ce/Ti)-2), 4 h ((UiO-66(Ce/Ti)-3), 5 h ((UiO-66(Ce/Ti)-4) and 24 h ((UiO-66(Ce/Ti)-5), respectively.

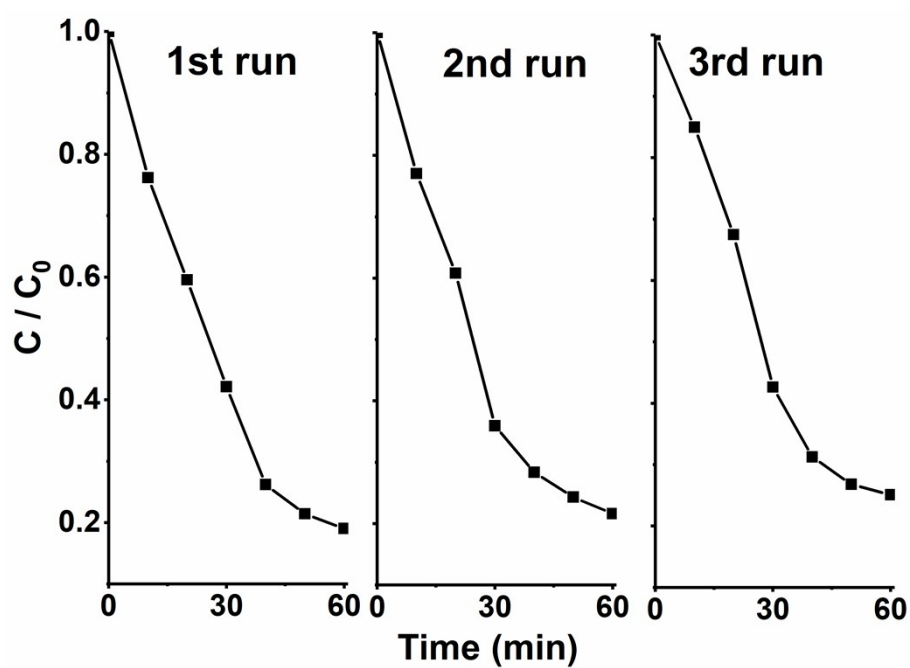


Figure S19 The time-evolving curve of TC degradation for three usage circles by using UiO-66(Ce/Ti) as the photocatalyst.

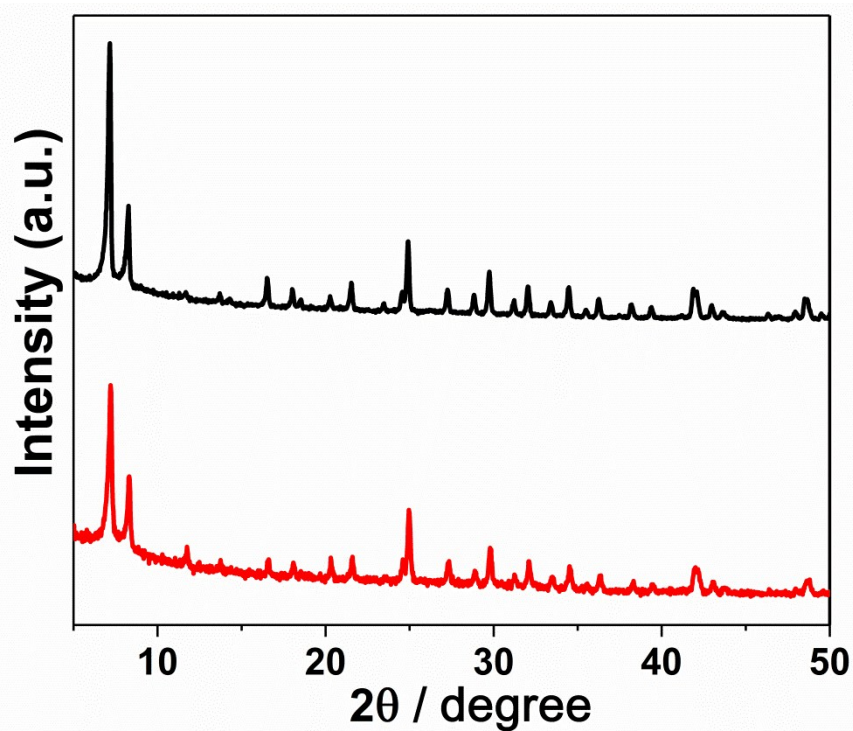


Figure S20 PXRD pattern of freshly prepared UiO-66(Ce/Ti) (black) and the UiO-66(Ce/Ti) collected after being used for three catalytic circles as the photocatalyst (red).

Reference

- 1 R. Liang, L. Shen, F. Jing, W. Wu, N. Qin, R. Lin and L. Wu, *Appl. Catal. B-Environ.*, 2015, **162**, 245.
- 2 Y. Ma, S. R. Pendlebury, A. Reynal, F. Le Formal and J. R. Durrant, *Chemical Science*, 2014, **5**, 2964.
- 3 (a) X. Zhang, Y. Yang, L. Song, J. Chen, Y. Yang and Y. Wang, *J. Hazard. Mater.*, 2019, **365**, 597; (b) X. Zhang, H. Li, X. Lv, J. Xu, Y. Wang, C. He, N. Liu, Y. Yang and Y. Wang, *Chem. Eur. J.*, 2018, **24**, 8822.
- 4 (a) R. D'Amato, A. Donnadio, M. Carta, C. Sangregorio, D. Tiana, R. Vivani, M. Taddei and F. Costantino, *ACS Sustain. Chem. Eng.*, 2019, **7**, 394; (b) Y. Wang, Y. Yang, N. Liu, Y. Wang and X. Zhang, *RSC Adv.*, 2018, **8**, 33096; (c) X. Zhang, X. Zhang, L. Song, F. Hou, Y. Yang, Y. Wang and N. Liu, *Int. J. Hydrogen Energy*, 2018, **43**, 18279.
- 5 M. Wells, D. L. Dermody, H. C. Yang, T. Kim, R. M. Crooks and A. J. Ricco, *Langmuir*, 1996, **12**, 1989.
- 6 Y. Yang, H. Dong, Y. Wang, C. He, Y. Wang and X. Zhang, *J. Solid State Chem.*, 2018, **258**, 582.